Negative piezoelectric response of van der Waals layered bismuth tellurohalides

Jinwoong Kim ⬤, Karin M. Rabe, and David Vanderbilt

Department of Physics and Astronomy, Rutgers University, Piscataway, New Jersey 08854-8019, USA

The polarization and piezoelectric response of the BiTeX (X = Cl, Br, and I) layered tellurohalides are computed from first principles. The results confirm a mixed ionic-covalent character of the bonding, and demonstrate that the internal structure within each triple layer is only weakly affected by the external stress, while the changes in the charge distribution with stress produce a substantial negative piezoelectric response. This suggests a mechanism for negative piezoelectric response that should remain robust even in the ultrathin film form in this class of materials.

I. INTRODUCTION

Conventional soft-mode ferroelectric materials exhibit a structural transition from a paraelectric to a polar phase as the temperature falls through a critical T_c, below which a polar-phonon mode freezes in to generate a ferroelectric ground state [1–3]. In general, this polar-phonon mode stiffens as the lattice constants are reduced, and consequently the magnitude of the polarization decreases with compressive strain. This corresponds to a positive piezoelectric response, $d_{33} > 0$, where by convention we consider the polar variant with $P > 0$. Recently, however, Liu and Cohen proposed a different mechanism by which materials can exhibit a negative piezoelectric response, and identified hexagonal ABC ferroelectrics as a class of materials in which the internal-strain contribution to the piezoelectricity is positive but small compared to the negative frozen-ion contribution, making the net piezoelectric response negative [4]. Negative piezoelectricity has also been experimentally demonstrated in ferroelectric polymers [5], organic molecular ferroelectric materials [6], and layered van der Waals ferroelectric materials [7,8].

BiTeX (X = Cl, Br, and I) compounds have attracted considerable recent interest as strongly polar quasi-2D materials. The breaking of inversion symmetry results from the layer geometry, in which a central Bi layer is neighbored by a Te layer on one side and a halide layer on the other side, forming a triple layer (TL) as shown in Fig. 1. The TLs are bonded to each other by weak van der Waals interactions, implying easy exfoliation and a soft mechanical response under uniaxial stress. The TLs are stacked so the Te layer is always on the same side of Bi, with one-TL periodicity resulting in a polar $P3m1$ space group for X = Br and I, and two-TL periodicity resulting in a polar $P6_3mc$ space group for X = Cl. Because of the strongly broken inversion symmetry combined with strong spin-orbit coupling, these materials are of interest for their large bulk Rashba effect, with potential spintronic applications [9–11]. BiTeI has also been much discussed for its topological properties, since it has been predicted to undergo a topological phase transition to a strong topological-insulator phase under pressure, mediated by a narrow but topologically robust Weyl semimetal phase [12–15], and to exhibit an enhanced nonlinear Hall conductivity [16].

The broken centrosymmetry of the crystal also naturally suggests the possibility of ferroelectricity or piezoelectricity. The polarization is not associated with a polar distortion of a nearby high-symmetry reference structure, and is inherently not switchable, since the bonding within the TL is much too strong to allow a structural reversal under applied electric field. However, as these systems are mechanically soft, there is a marked change in structure under applied stress, which can be expected to result in a change in polarization and corresponding piezoelectric response.

In this paper, we investigate the electric polarization and piezoelectric response of BiTeX by using first-principles calculations. We compare the calculated dipole moments with two plausible models that anticipate opposite directions of the dipole moment, deciding in favor of the one that treats the BiTe unit as more covalently than ionically bonded. We will see that, while structurally, the BiTeX TLs behave as relatively rigid units, internal charge rearrangement under applied uniaxial strain or stress leads to a substantial negative piezoelectric response. This suggests a mechanism of piezoelectricity that may be widely applicable to a broad class of insulating materials based on layered van der Waals stacking of polar constituents.

II. METHODS

The polarization and piezoelectric response of BiTeX are determined from first-principles calculations carried out using the VASP package [17,18]. The pseudopotentials are of the projector-augmented-wave type as implemented in VASP [19,20], with valence configurations $6s^2 6p^3$ for Bi, $5s^2 5p^4$ for Te, and $3s^2 3p^5$, $4s^2 4p^5$, and $5s^2 5p^5$ for Cl, Br, and I, respectively. The exchange-correlation functional is described by the modified Perdew-Burke-Ernzerhof generalized gradient approximation for solids (PBEsol) [21]. The plane-wave cut-off energy is set to 400 eV. The Brillouin zone sampling grid is 12 × 12 ×8 for the 1-TL periodic $P3m1$ structure and 12 × 12 ×4 for the 2-TL periodic $P6_3mc$ structure; relative energy differences between the two structures were obtained by computing both in the doubled-cell structure with the 12 × 12 ×4 grid. Spin-orbit coupling is included in all
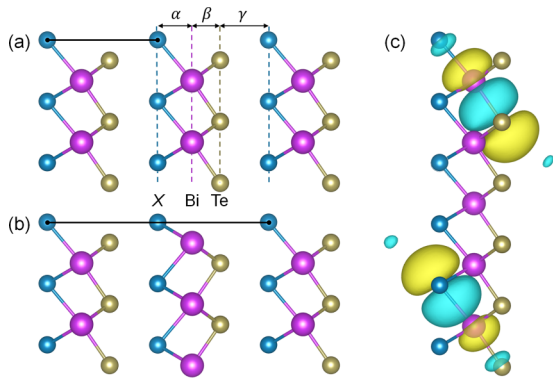
FIG. 1. Layered structure of BiTeX for (a) $X = $ I or Br in the $P3m1$ structure, and (b) $X = $ Cl in the doubled-cell $P6_3mc$ structure. Horizontal solid lines indicate c lattice constants. Distances α and β denote Bi-X and Bi-Te intralayer distances, while γ is the separation between triple layers. (c) Wannier functions constructed from p bands, having Bi-X (lower) and Bi-Te (upper) bond-orbital character.

calculations. The structural coordinates are relaxed within a force threshold of 1.5 meV/Å. The electric polarization is computed using the Berry-phase method [22,23], and the Wannier charge centers [24] are obtained using the VASP-WANNIER90 interface [25]. The maximal localization of the Wannier functions is carried out separately for the s and p bands to avoid sp_3 hybridization.

For a crystal composed of weakly coupled molecules or layers, it is natural to compute the polarization from the dipole moment of the individual unit. For a periodic system, this value can be quantitatively obtained by computing the Berry phase polarization [2,22,23], where the branch choice arising from the quantum of polarization can be resolved by choosing the value closest to that estimated by the dipole moment integral or by using the Wannier center formulation and choosing the Wannier centers to be within the individual unit. In this paper, we consider only $p = p_3$, the dipole moment per the unit cell measured along the stacking direction $\hat{e}_3$, and adopt the convention that the polarization P_3, electric field $\mathcal{E}_3$, strains $\eta_3 = c/c_0 - 1$, and stresses σ_3 (Voigt notation for η and σ), will also be written without the subscript for simplicity.

We calculate various piezoelectric responses following the standard definitions [26–28]. The piezoelectric stress tensor elements $e_{\alpha j}$ are defined in terms of the derivative of stress with respect to the electric field, or equivalently, polarization with respect to strain,

$$e_{\alpha j} = -\frac{\partial \sigma_j}{\partial \mathcal{E}_\alpha}\bigg|_\eta = \frac{\partial P_\alpha}{\partial \eta_j}\bigg|_\mathcal{E}, \qquad (1)$$

while the piezoelectric strain tensor elements $d_{\alpha j}$ are related to the derivative of strain with electric field, or equivalently, the derivative of polarization with respect to stress:

$$d_{\alpha j} = -\frac{\partial \eta_j}{\partial \mathcal{E}_\alpha}\bigg|_\sigma = \frac{\partial P_\alpha}{\partial \sigma_j}\bigg|_\mathcal{E}. \qquad (2)$$

To calculate the piezoelectric stress response, the polarization P is calculated on a grid of strains η with the in-plane lattice constant fixed to the zero-stress value, and is fitted to a polynomial to obtain the derivative corresponding to the

TABLE I. Calculated structural parameters of BiTeX ($X = $ I, Br, Cl). V is cell volume, a and c are in-plane and out-of-plane lattice constants, α and β are Bi-X and Bi-Te layer spacings, and P is polarization. The prime on BiTeCl$'$ denotes the results for the same $P3m1$ structure as for $X = $ I and Br; the unprimed version is for the ground-state $P6_3mc$ structure.

	V (Å^3)	a (Å)	c (Å)	α (Å)	β (Å)	P (C/m^2)
BiTeI	111.5	4.343	6.823	2.104	1.721	0.069
BiTeBr	102.6	4.270	6.499	1.871	1.754	0.100
BiTeCl$'$	97.5	4.235	6.275	1.677	1.767	0.107
BiTeCl	195.5	4.239	12.563	1.667	1.765	0.099

piezoelectric response e_{33}. For the same grid of strains η, we compute the optimized value of a at each η, and then using the values of stress and polarization reported by VASP at each η, we fit the results to extract the value of the piezoelectric d_{33} coefficient. In addition, we compute a mixed response d_{33}^{epi} by carrying out a similar fitting procedure but at fixed in-plane lattice constant.

III. RESULTS

A. Structure and polarization

BiTeI and BiTeBr crystallize in the hexagonal structure illustrated in Fig. 1(a), space group $P3m1$ (No. 156), with three atoms per cell. BiTeCl has the same internal layer structure, but alternate TLs are rotated $180°$ about $\hat{e}_3$ on an axis passing through the X atom, as shown in Fig. 1(b), resulting in a doubled six-atom unit cell belonging to space group $P6_3mc$ (No. 186).

Our computed structural parameters for these three materials, together with the Berry-phase polarization P, are given in Table I. In the case of $X = $ Cl, we carried out calculations in both the $P3m1$ and $P6_3mc$ structures; the former is designated with a prime (BiTeCl$'$) as a reminder that it is not the experimental ground-state structure. We see rather obvious trends in that the volume and the Bi-X distance α shrink as X becomes more electronegative, while the Bi-Te distance β remains roughly constant. The trend in going to $X = $ Cl is most consistent when the same structure is assumed (first three rows of the table). The change to the doubled-cell $P6_3mc$ in the last row is generally small, showing that the stacking sequence does not have a strong effect on the structural parameters.

The calculated c lattice constant of BiTeI is close to the experimental value of 6.854 Å [29]. We tested several different exchange-correlation potentials including some with van der Waals corrections, but we find that our use of PBEsol produces the closest agreement for the c lattice constant, with an error of 0.5%, compared to the other ones we tested (5.9% for PBE [30], 3.7% for PBE+TS [31], and 2.2% for SCAN [32]). This is consistent with a previous theoretical report [11] in which the PBEsol functional was found to give the most accurate prediction of the BiTeX structure.

We computed the ground-state energies for each of the materials in both the $P3m1$ and $P6_3mc$ structures, finding that the doubled-cell $P6_3mc$ structure is higher in energy by 7.3, 4.8, and 5.1 meV for BiTeI, BiTeBr, and BiTeCl,

respectively. This correctly predicts the 1-TL ground state structure for BiTeI and BiTeBr, but it does not account for the observation of the 2-TL structure of BiTeCl. However, the energy differences are small, and are near the limit of our first-principles resolution. We speculate that it may be necessary to take differences in vibrational entropy into account to explain the observed structure of BiTeCl. In any case, as noted above, a comparison of the BiTeCl and BiTeCl′ results in Table I shows that the structural properties are not very sensitive to the choice of space-group structure, and we report results for BiTeCl in both structures.

Figure 1(c) shows two of the maximally localized Wannier functions constructed from the p bands of BiTeI, rendered using the VESTA software package [33]. We see a somewhat asymmetric bond orbital composed of Bi and X p orbitals at the bottom, and a somewhat more symmetric bond orbital made of Bi and Te p orbitals at the top. Both show significant covalent bonding, but the greater asymmetry of the Bi-X bond orbital is consistent with a stronger ionic character, as expected from the stronger electronegativity of the halide X atom. The trend in the strength of covalency is also evident from the values of α and β reported in Table I. Not surprisingly, the β value (Bi-Te spacing) remains roughly constant, while the α value (Bi-X spacing) shrinks significantly in going from X = I to Br to Cl, with the increasing electronegativity of the X ion.

In view of the soft mechanical response, it is of interest to ask what would happen in the limiting case of much larger tensile strains. We find that the system becomes mechanically unstable for strains above about 8%, after which the dipole moment rapidly saturates to its free-space value. However, it appears doubtful that inter-TL separations on this order could be achieved in practice, since the electric field needed to induce such a large piezoelectric response would exceed typical dielectric breakdown fields.

The results for the electric polarization for each of the three materials, computed using the Berry-phase approach as described in the Methods section, are presented in the last column of Table I. Not surprisingly, the polarization, being a dipole moment per unit volume, increases as the volume decreases, but this does not account for all of the variation. The interpretation of the sign and magnitude of the polarization is the topic of the next subsection.

B. Interpretation of the polarization

The computed polarization reported in Table I is positive, so the dipole moment of the layers points along the direction from the halide to the Te. Surprisingly, two simple models, shown in Figs. 2(a) and 2(b), predict opposite signs of the polarization. Model A, the fully ionic model shown in Fig. 2(a), assumes that the ions keep their nominal valence, in which case the dipole moment is estimated as

$$p_{\mathrm{A}} = e(\alpha - 2\beta). \tag{3}$$

(recall that α and β are the Bi-X and Bi-Te layer spacings, respectively). From the figure, it is clear that the dipole moment would then point to the left (negative, in our convention) because of the excessive negative charge of Te^{-2} compared to X^-.
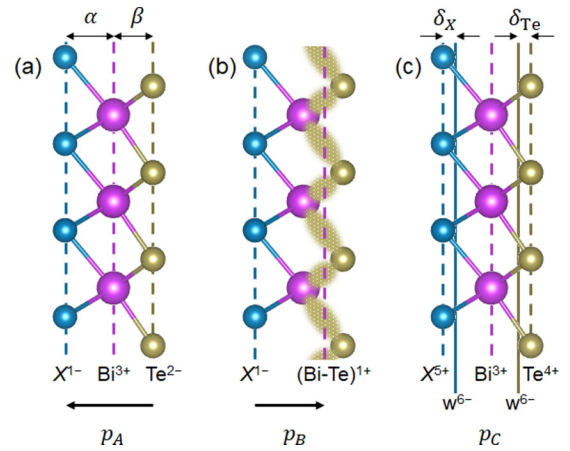

FIG. 2. (a), (b) Schematic view of two simple models of the polarization in BiTeX. (a) Fully ionic model suggests a negative dipole moment. (b) Model with a covalent Bi-Te unit suggests a positive dipole moment. (c) Wannier function perspective. Solid vertical lines indicate Wannier center locations, with $\delta_{X,\mathrm{Te}}$ denoting their displacements relative to the neighboring anion layers (dotted vertical lines).

Model B, shown in Fig. 2(b), assumes a strong covalent bond between neighboring Bi and Te layers, and treats this pair of layers as a single unit with an overall valence of $+1$. The dashed vertical line at right in Fig. 2(b) indicates an average position of this Bi-Te unit, taken to be midway between the Bi and Te planes. In this model the dipole is predicted to be

$$p_{\mathrm{B}} = e(\alpha + \beta/2), \tag{4}$$

which is clearly positive, in contrast with the prediction of the previous model.

Table II reports the values of the dipole moment as computed from first principles (p_{DFT}), as well as the values computed from models A and B. Neither of these models gives a value for the dipole that is close to the first-principles value. The first-principles result is not far from an average of the two, suggesting that models A and B can be taken as describing two end points corresponding to extreme ionic and mixed ionic-covalent bonding states, respectively.

As described in Sec. II, the polarization is given exactly in terms of the coordinates of the ions and those of the Wannier centers of the occupied bands. The positions of the Wannier

TABLE II. Dipole moment of the triple atomic layer in bulk BiTeX, in units of e Å, for the three models in Fig. 2. Last two columns give the values of δ_X and δ_{Te}, describing the displacements of the p-band Wannier centers from nearby ionic planes, in units of Å. BiTeCl′ refers to the same $P3m1$ structure as for X = I and Br, although it is not the observed ground state for X = Cl.

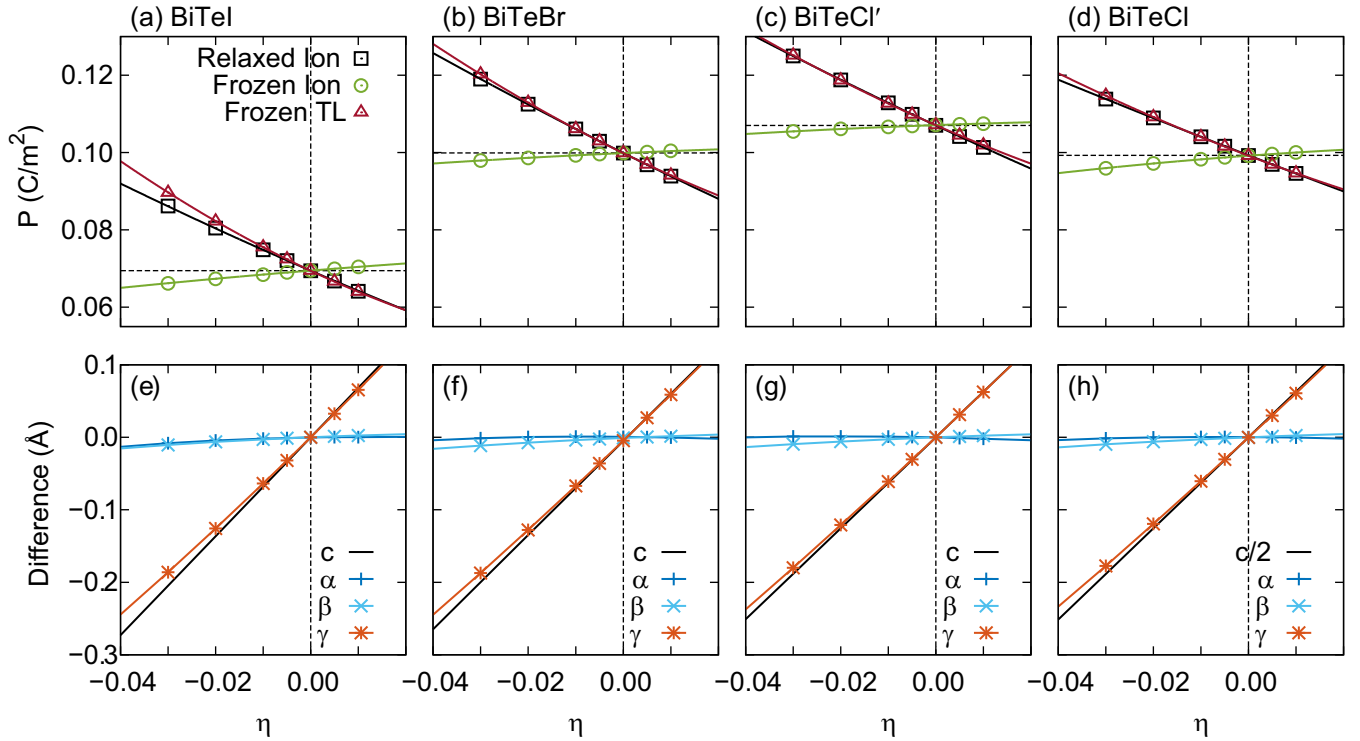|	p_{DFT}	p_{A}	p_{B}	p_{c}	δ_X	δ_{Te}
BiTeI	0.48	−1.34	2.96	0.43	0.24	0.54
BiTeBr	0.64	−1.64	2.75	0.56	0.19	0.55
BiTeCl′	0.61	−1.86	2.56	0.57	0.15	0.55
BiTeCl	0.61	−1.86	2.55	0.53	0.15	0.55

FIG. 3. (a)–(d) Calculated polarization vs strain $\eta = c/c_0 - 1$ of BiTeX at fixed in-plane lattice constant for relaxed-ion, frozen-ion, and frozen-triple-layer cases. Solid lines are fits whose slopes at equilibrium ($\eta = 0$, dashed vertical line) correspond to e_{33}. (e)–(h) Changes of relaxed structural parameters under uniaxial strain. Here α and β are the Bi-X and Bi-Te internal atomic interlayer distances (see Fig. 1); γ is inter-triple-layer spacing.

centers constructed from the occupied p bands, shown earlier in Fig. 1(c), are indicated by the solid vertical lines in Fig. 2(c). This approach would be exact if the information on the Wannier centers constructed from the occupied s bands were included as well, but we assume these to coincide with the atomic coordinates; this is a reasonable approximation since the s bands are well separated and weakly hybridized with other bands. There are thus two additional parameters taken from first principles, namely the shifts δ_X and δ_{Te}, relative to the anion coordinates, of the Wannier centers constructed from the occupied p bands. We then include the s charge $-2e$ into our definition of the core charges, which become $+4$, $+3$, and $+5$ for Te, Bi, and X, respectively. The remaining 12 electrons form anion p-like Wannier functions whose Wannier-center positions are illustrated in Fig. 2(c). Six of these are associated with Wannier centers displaced by δ_{Te} from the Te centers, and the other six are centered a distance δ_X from the X centers, measured along the z direction. Accounting for all of the ionic and Wannier contributions shown in Fig. 2(c), the dipole moment is given by

$$p_C/e = -5\alpha + 4\beta + 6(\alpha - \delta_X) - 6(\beta - \delta_{TE})$$
$$= \alpha - 2\beta - 6(\delta_X - \delta_{Te}), \tag{5}$$

and comparing with Eq. (3), this is just

$$p_C = p_A + 6e(\delta_{Te} - \delta_X). \tag{6}$$

Turning to the results given in Table II, we see that this analysis agrees well with the full density functional theory

(DFT) results. We can now think of model A as a limit in which $\delta_{Te} - \delta_X = 0$, and model B as corresponding to $\delta_{Te} - \delta_X = 5\beta/12$. From Tables I and II, we get $\delta_{Te} - \delta_X$ are 2.1, 2.5, and 2.7 in units of $\beta/12$ for $X=$I, Br, and Cl, respectively, indicating neither is a good approximation. From another point of view, we can say that an accurate picture of the dipole is given by modifying model A according to Eq. (6). Note, however, that δ_{Te} is much larger than δ_X in Table II, as expected given the stronger covalency of the Bi-Te bonding, as was discussed toward the end of Sec. III A when describing the Wannier functions shown in Fig. 1(c). Thus, Eq. (6) leads to a large positive correction to the prediction of model A.

C. Piezoelectric response at fixed in-plane lattice constant

1. Piezoelectric stress coefficients

Figures 3(a)–3(d) show the polarization of BiTeX as a function of uniaxial strain at fixed in-plane lattice constant. These values are labeled relaxed ions since they include full structural relaxation. The slopes at the equilibrium state correspond to the piezoelectric stress tensor elements e_{33}, which are reported as the relaxed-ion (RI) values in the first column of Table III. The values are strongly negative for all three materials.

In the theory of piezoelectricity, it is often instructive to separate the strain-induced change in polarization into a contribution directly generated by the change in strain and a contribution due to the strain-induced change in polar lattice distortion [4]. In 3D bulk crystals, this is done by first

TABLE III. Calculated piezoelectric responses of BiTeX materials: e_{33} for relaxed-ion (RI), frozen-ion (FI), and frozen-triple-layer (FTL) cases; and proper, improper, and epitaxial d_{33} piezoelectric responses. The in-plane-lattice constants are relaxed for proper and improper d_{33} cases and fixed otherwise. BiTeCl$'$ refers to the same $P3m1$ structure as for X = I and Br, although it is not the observed ground state for X = Cl.

	e_{33} (C/m^2)			d_{33} (pm/V)		
	RI	FI	FTL	Prop.	Imp.	Epi.
BiTeI	-0.53	0.10	-0.57	-24.4	-23.0	-24.4
BiTeBr	-0.61	0.06	-0.60	-30.6	-28.6	-31.2
BiTeCl$'$	-0.57	0.04	-0.54	-34.6	-32.4	-35.9
BiTeCl	-0.47	0.09	-0.47	-27.6	-25.1	-29.7

computing the change in polarization with a "frozen-ion" constraint corresponding to uniform scaling of the atomic positions in the unit cell as the strain state is changed. The "internal-strain" contribution is then the subsequent change in polarization as the polar distortion, with associated changes in other internal structural parameters, is changed to its final value.

In quasi-2D systems, we use a different decomposition, based on the concept that the change in strain state in these systems is accomplished primarily by changing the spacing between the 2D layers, keeping the internal structure of the layers "frozen." This can be understood as arising from the weak van der Waals bonding between 2D layers, in contrast to the much stronger covalent bonding within the 2D layers. In the present case, the changes of the ionic coordinates presented in Figs. 3(e)–3(h) show that the Bi-X and Bi-Te interlayer spacings (α and β) are almost constant as a function of η, while the changes in the inter-TL spacing tracks very closely with the c lattice constant. The polarizations obtained from the frozen-TL model are shown as the triangles in Figs. 3(a)–3(d), and the e_{33} values are given in the FTL column of Table III. These are in excellent agreement with the full first-principles (RI) results, both in sign and magnitude. The internal-strain contribution due to strain-induced change in the structure of the TL is thus very small. We note that a small internal-strain contribution is also characteristic of the negative piezoelectric response of the 3D hexagonal ABC compounds discussed in Ref. [4].

We can compare this quasi-2D decomposition with the decomposition used in the 3D bulk crystal case [Figs. 3(a)–3(d)]. After uniform scaling, the change in internal structural parameters is substantial and not just an adjustment of a polar mode. The computed frozen-ion change in polarization is thus much smaller and has the opposite sign compared to the total change in polarization, so this decomposition does not give useful physical insight to the piezoelectric response.

It is important to note that the frozen-TL model does not imply a fixed dipole for the TL, as electronic relaxation occurs self-consistently at each value of c. If the dipole of the frozen TL were independent of c, then the negative piezoelectric response would be described as coming from a simple volume effect, where the change in $P = p/V$ is mainly a result of the change in V, with the result that a compression or expansion simply concentrates or dilutes the polarization. More

TABLE IV. Decomposition of the piezoelectric response into two contributions as given in Eq. (7). All quantities in units of C/m^2.

	$-p_0/V_0$	$V_0^{-1}(\partial p/\partial \eta)$	e_{33}
BiTeI	-0.069	-0.460	-0.53
BiTeBr	-0.100	-0.507	-0.61
BiTeCl$'$	-0.107	-0.464	-0.57
BiTeCl	-0.099	-0.374	-0.47

generally, the change in dipole can be taken into account by writing

$$e_{33} = \frac{\partial}{\partial \eta}(V^{-1}p)_{\eta=0}$$

$$= -\frac{p_0}{V_0} + \frac{1}{V_0}\frac{\partial p}{\partial \eta}\bigg|_{\eta=0}, \tag{7}$$

where p_0 and V_0 are the dipole moment and cell volume at $\eta = 0$. If the polarization p of the frozen TL were independent of η, then only the first term would be present. This purely mechanical model, based only on the change of volume, does correctly predict the negative sign of the piezoelectric response, but we find that it severely underestimates the magnitude of the effect.

To investigate this, we have calculated the dependence of the Wannier-center shifts δ_{Te} and δ_X on the uniaxial strain η, since these are the parameters that reflect the internal change of the TL dipole that is not captured by the structural coordinates alone. In the purely mechanical limit, δ_{Te} and δ_X would be independent of η, and the second term in Eq. (7) could be dropped. We find that δ_{Te} is indeed very nearly independent of η; it varies by only about 0.1% with a 1% change in c. By contrast, we find a much more significant change in the position of the centers of the Bi-X Wannier functions, with δ_X changing by about 2.3, 2.6, and 2.1% for X=I, Br, and Cl, respectively, for every 1% change in c. We can rationalize this change by noting that the halogen environment becomes more symmetric (less distinction between intra-TL and inter-TL neighbor distances), so that the Wannier center shifts toward the X coordinate, as the TLs are pressed closer to each other. An inspection of the changes of the Wannier functions (not shown) does indicate a stronger X-Te hybridization across the van der Waals gap, consistent with a reduction of δ_X, as the distance between TLs is decreased.

In short, we find that the negative piezoelectric response arises mainly from an electronic effect, namely the change of magnitude of the TL dipole with compression, which comes about because of the change in δ_X values as the TLs are pressed together. This is reminiscent of the conclusions of Liu and Cohen, who also found that an electronic response (at fixed internal coordinates in their case) was crucial for obtaining the negative piezoelectricity in the ABC ferroelectrics [4]. The consequences of this are summarized in Table IV, where the contributions of the first and second terms in Eq. (7) are given independently, clarifying their relative contribution to the piezoelectric response e_{33}. It now becomes clear that while the purely mechanical model, represented by $-p_0/V_0$, correctly gives the negative sign of the piezoelectric response, it underestimates the magnitude of the response by
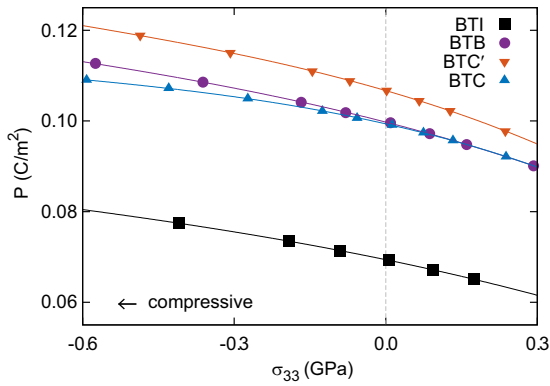
FIG. 4. Calculated polarization of BiTeX vs uniaxial stress at relaxed in-plane lattice constant. Solid lines are fits whose slopes at equilibrium ($\sigma_{33} = 0$, dashed vertical line) correspond to d_{33}.

almost an order of magnitude. The modulation of the dipolar contribution of the Bi-X bond with compression provides a large boost to the observed effect, and is responsible for the unexpectedly large piezoelectric effect that is revealed by our calculations.

2. Piezoelectric strain coefficients

Next, we consider the piezoelectric strain response d_{33}. Because this is defined under zero-stress boundary conditions, the unit cell area now varies with σ, and there is a distinction between proper and improper piezoelectric responses [34]. The "improper" piezoelectric response $d_{33}^{\text{imp}} = \partial P/\partial \sigma$ simply describes the change of polarization under stress. However, the piezoelectric response is typically measured by tracking the stress-induced current flowing between top and bottom electrodes in a capacitor configuration, which corresponds to the change of surface charge per unit cell $\tilde{P} = AP$ with external stress, where A is the cell area. This defines the "proper" piezoelectric response, where the two are related by

$$d_{33}^{\text{prop}} = \frac{1}{A}\frac{\partial \tilde{P}}{\partial \sigma} = \frac{P}{A}\frac{\partial A}{\partial \sigma} + d_{33}^{\text{imp}}. \tag{8}$$

Figure 4 shows the variation of P with respect to the uniaxial stress σ_3; the slope at $\sigma_3 = 0$ yields d_{33}^{imp}. A corresponding analysis of the dependence of $\tilde{P}$ on uniaxial stress gives d_{33}^{prop}, and the results are summarized in Table III. The improper response ranges from -23 pm/V to -32 pm/V, which systematically increases in magnitude from X=I to Br to Cl$'$ in the same $P3m1$ structure. The change of structure (Cl$'$ to Cl) gives a $\sim$20% reduction, resulting in the Br compound having the largest d_{33}^{imp} response. The correction term expressing the difference between d_{33}^{prop} and d_{33}^{imp} in Eq. (8), whose sign is negative (the cell area expands under uniaxial compression along c), enhances the negative piezoelectric responses slightly, by $\sim$5-9% compared to improper responses. As a result, the proper piezoelectric response of BiTeBr reaches -30 pm/V.

3. Epitaxial piezoelectric coefficients

Finally, we calculated the mixed response d^{epi} (see the Methods section), defined under conditions of fixed in-plane

strain and out-of-plane stress. Here there is once again no distinction between proper and improper responses. The results are given in the last column of Table III. The changes are not very dramatic; d_{33}^{epi} is similar to d_{33}^{prop} for $X = $ I and slightly larger for the Br, Cl$'$, and Cl cases. We have checked the effect of a fixed in-plane lattice constant that is set to a modified value, as in the case of coherent heteroepitaxy on a substrate. A compressive epitaxial strain is found to induce a negligible change, whereas a tensile epitaxial strain reduces the magnitude of the d_{33}^{epi} response somewhat, especially for $X = $ Cl$'$ and Cl.

D. Discussion

To review, we have shown that the physics of the piezoelectric response in the BiTeX system is very different from that of conventional ferroelectrics such as perovskite oxides. In those systems, the proximity to a polar instability, the associated soft polar modes, and the anomalously large dynamical effective charges generate very strong piezoelectric responses. Here, instead, we start with a system that is far from any structural phase transition, so it might be expected to show quite a small piezoelectric response.

Nevertheless, we find a substantial piezoelectric response in the BiTeX system. Our theory shows that a model in which the internal structure of each TL is frozen, and only the spacing between them changes, gives an excellent account of the structural changes under applied uniaxial strain. If the dipole moment of the TL were also frozen, this would already account for the anomalous negative sign of the piezoelectric response. However, we find that the electronic charge redistribution within the TL plays a very important role, and is responsible for the surprisingly large e_{33} values.

To be sure, our calculated $|e_{33}|$ values of $\sim$0.50 C/m^2 are smaller, by an order of magnitude or more, than those of well-known perovskites such as PbTiO$_3$ and PZT, which have values in the range of 4-12 C/m^2. However, it is still comparable to that of wurtzite semiconductors (0.02–1.5 C/m^2) and *ABC* ferroelectric materials (0.4–1.5 C/m^2) [4,35]. AlN and LiMgAs are reported to have the largest e_{33} responses of $\sim$1.5 C/m^2 among each class of materials [4,35], which is slightly larger than the classical wurtzite piezoelectric material ZnO having $e_{33} \simeq 1.2$ C/m^2 [28,36], and only a factor of 3 larger than that of BiTeX. The most negative e_{33} among the *ABC* ferroelectrics is found in NaZnSb as $e_{33} = -1.04$ C/m^2, only twice larger than BiTeX. A theoretical investigation of the negative piezoelectric responses in the *ABC* ferroelectrics has revealed that the frozen-ion $\bar{e}_{33}$ gives a negative contribution that dominates the total response [4]. This is in a sharp contrast with BiTeX, where the frozen-ion contribution is rather small and positive.

Moreover, the piezoelectric response of BiTeX is further magnified when converting to the piezoelectric strain coefficient d_{33} because of the softness of the interlayer van der Waals interaction, which implies a large strain per applied uniaxial stress. This makes the comparison of the d_{33} values of the BiTeX materials even closer to being competitive with other piezoelectrics. Our calculated $|d_{33}|$ values, in the range of 24-36 pm/V, compare well to those of LiMgP (25 pm/V) and LiMgAs (29 pm/V), which have the most positive d_{33}

among the *ABC* ferroelectric materials, even though their e_{33} values are a factor of 3 larger as discussed above [4]. The relative enhancement of d_{33} relative to e_{33} in BiTe*X* is also evident by comparison with BaTiO$_3$ [28], where $|e_{33}| = 4.44$ C/m^2 is an order of magnitude larger than for BiTe*X*, while $|d_{33}| = 14.7$ pm/V is a factor of 2 smaller than for BiTe*X*.

Recent studies have shown that ultrahigh piezoelectric responses have been achieved with d_{33} up to 2800 pm/V in PMN-PT [37,38] and 640 pm/V in BaTiO$_3$-based ceramic systems, [39,40] and a negative piezoelectric response of $d_{33} = -690$ pm/V has been reported in the class of ferroelectric polymers based on polyvinylidene difluoride (PVDF) [40,41]. We note, however, that these ultrahigh piezoelectric responses are a result of careful compositional tuning of the system. For example, the simple β phase of PVDF exhibits a d_{33} of -50 pm/V, which is only a factor of 2 larger than for BiTe*X* [40,42].

We also note that the d_{33} responses of BiTe*X* are comparable to the values reported for some thin-film PZT samples (21.3 pm/V) [43], although still an order of magnitude smaller than for thick-film PZT (457 pm/V). Because the mechanism of piezoelectricity in the BiTe*X* system is completely independent of any soft-mode transition, there is no reason to expect our computed responses to suffer from the kind of finite-size effects that suppress the piezoelectricity in thin-film geometries for conventional materials. Taken together with our encouraging estimates of the size of the responses reported above, these results suggest that the BiTe*X* materials could

provide a promising alternative material system to use as a basis for microactuator and other specialized applications.

IV. SUMMARY

We have used first-principles methods to calculate the polarizations and piezoelectric responses of BiTe*X* for $X =$ Cl, Br, I. The piezoelectric response is found to be negative. The change in structure under uniaxial stress is described to an excellent approximation by a "frozen TL" model in which the BiTe*X* unit is internally rigid, while the spacing between these units is modulated by the applied uniaxial strain. However, the dipole moment of the TL is not frozen, and changes with stress due to electronic relaxation are found to dominate the piezoelectric response. The piezoelectric responses are an order of magnitude smaller than those of commercial bulk piezoelectric materials, but the mechanism can be expected to survive in the thin-film limit where standard piezoelectrics tend to degrade. Thus, BiTe*X* could be a promising alternative material for thin-film piezoelectric devices. The recent explosion of interest in stacked van-der-Waals–bonded heterostructures provides opportunities for BiTe*X* as a piezoelectric component in such systems.

[1] G. H. Haertling, J. Am. Ceram. Soc. **82**, 797 (1999).

[2] R. Resta, Rev. Mod. Phys. **66**, 899 (1994).

[3] M. Dawber, K. M. Rabe, and J. F. Scott, Rev. Mod. Phys. **77**, 1083 (2005).

[4] S. Liu and R. E. Cohen, Phys. Rev. Lett. **119**, 207601 (2017).

[5] I. Katsouras, K. Asadi, M. Li, T. B. van Driel, K. S. Kjær, D. Zhao, T. Lenz, Y. Gu, P. W. M. Blom, D. Damjanovic, M. M. Nielsen, and D. M. de Leeuw, Nat. Mater. **15**, 78 (2015).

[6] I. Urbanaviciute, X. Meng, M. Biler, Y. Wei, T. D. Cornelissen, S. Bhattacharjee, M. Linares, and M. Kemerink, Mater. Horiz. **6**, 1688 (2019).

[7] L. You, Y. Zhang, S. Zhou, A. Chaturvedi, S. A. Morris, F. Liu, L. Chang, D. Ichinose, H. Funakubo, W. Hu, T. Wu, Z. Liu, S. Dong, and J. Wang, Sci. Adv. **5**, eaav3780 (2019).

[8] S. M. Neumayer, E. A. Eliseev, M. A. Susner, A. Tselev, B. J. Rodriguez, J. A. Brehm, S. T. Pantelides, G. Panchapakesan, S. Jesse, S. V. Kalinin, M. A. McGuire, A. N. Morozovska, P. Maksymovych, and N. Balke, Phys. Rev. Mater. **3**, 024401 (2019).

[9] K. Ishizaka, M. S. Bahramy, H. Murakawa, M. Sakano, T. Shimojima, T. Sonobe, K. Koizumi, S. Shin, H. Miyahara, A. Kimura, K. Miyamoto, T. Okuda, H. Namatame, M. Taniguchi, R. Arita, N. Nagaosa, K. Kobayashi, Y. Murakami, R. Kumai, Y. Kaneko, Y. Onose, and Y. Tokura, Nat. Mater. **10**, 521 (2011).

[10] M. S. Bahramy, R. Arita, and N. Nagaosa, Phys. Rev. B **84**, 041202(R) (2011).

[11] B. Monserrat and D. Vanderbilt, Phys. Rev. Mater. **1**, 054201 (2017).

[12] S. Murakami, New J. Phys. **9**, 356 (2007).

[13] M. S. Bahramy, B.-J. Yang, R. Arita, and N. Nagaosa, Nat. Commun. **3**, 679 (2012).

[14] J. Liu and D. Vanderbilt, Phys. Rev. B **90**, 155316 (2014).

[15] S. Murakami, M. Hirayama, R. Okugawa, and T. Miyake, Sci. Adv. **3**, e1602680 (2017).

[16] J. I. Facio, D. Efremov, K. Koepernik, J.-S. You, I. Sodemann, and J. van den Brink, Phys. Rev. Lett. **121**, 246403 (2018).

[17] G. Kresse and J. Furthmüller, Phys. Rev. B **54**, 11169 (1996).

[18] G. Kresse and J. Furthmüller, Comput. Mater. Sci. **6**, 15 (1996).

[19] P. E. Blöchl, Phys. Rev. B **50**, 17953 (1994).

[20] G. Kresse and D. Joubert, Phys. Rev. B **59**, 1758 (1999).

[21] J. P. Perdew, A. Ruzsinszky, G. I. Csonka, O. A. Vydrov, G. E. Scuseria, L. A. Constantin, X. Zhou, and K. Burke, Phys. Rev. Lett. **100**, 136406 (2008).

[22] R. D. King-Smith and D. Vanderbilt, Phys. Rev. B **47**, 1651 (1993).

[23] D. Vanderbilt and R. D. King-Smith, Phys. Rev. B **48**, 4442 (1993).

[24] N. Marzari, A. A. Mostofi, J. R. Yates, I. Souza, and D. Vanderbilt, Rev. Mod. Phys. **84**, 1419 (2012).

[25] A. A. Mostofi, J. R. Yates, G. Pizzi, Y.-S. Lee, I. Souza, D. Vanderbilt, and N. Marzari, Comput. Phys. Commun. **185**, 2309 (2014).

[26] A. Ballato, IEEE Trans. Sonics Ultrason. **42**, 916 (1995).

[27] J. F. Nye, *Physical Properties of Crystals Their Representation by Tensors and Matrices* (Clarendon Press, Oxford, 2012).

[28] X. Wu, D. Vanderbilt, and D. R. Hamann, Phys. Rev. B **72**, 035105 (2005).

[29] A. Shevelkov, E. Dikarev, R. Shpanchenko, and B. Popovkin, J. Solid State Chem. **114**, 379 (1995).

[30] J. P. Perdew, K. Burke, and M. Ernzerhof, Phys. Rev. Lett. **77**, 3865 (1996).

[31] A. Tkatchenko and M. Scheffler, Phys. Rev. Lett. **102**, 073005 (2009).

[32] J. Sun, A. Ruzsinszky, and J. P. Perdew, Phys. Rev. Lett. **115**, 036402 (2015).

[33] K. Momma and F. Izumi, J. Appl. Crystallogr. **44**, 1272 (2011).

[34] D. Vanderbilt, J. Phys. Chem. Solids **61**, 147 (2000).

[35] F. Bernardini, V. Fiorentini, and D. Vanderbilt, Phys. Rev. B **56**, R10024 (1997).

[36] M. Catti, Y. Noel, and R. Dovesi, J. Phys. Chem. Solids **64**, 2183 (2003).

[37] S.-E. Park and T. R. Shrout, J. Appl. Phys. **82**, 1804 (1997).

[38] Q. Zhou, K. H. Lam, H. Zheng, W. Qiu, and K. K. Shung, Prog. Mater. Sci. **66**, 87 (2014).

[39] J. P. Praveen, T. Karthik, A. James, E. Chandrakala, S. Asthana, and D. Das, J. Eur. Ceram. Soc. **35**, 1785 (2015).

[40] H. Wei, H. Wang, Y. Xia, D. Cui, Y. Shi, M. Dong, C. Liu, T. Ding, J. Zhang, Y. Ma, N. Wang, Z. Wang, Y. Sun, R. Wei, and Z. Guo, J. Mater. Chem. C **6**, 12446 (2018).

[41] S. K. Ghosh, T. K. Sinha, B. Mahanty, and D. Mandal, Energy Technol. **3**, 1190 (2015).

[42] N. Soin, D. Boyer, K. Prashanthi, S. Sharma, A. A. Narasimulu, J. Luo, T. H. Shah, E. Siores, and T. Thundat, Chem. Commun. **51**, 8257 (2015).

[43] Q. Guo, G. Z. Cao, and I. Y. Shen, J. Vib. Acous. **135**, 011003 (2013).